Spatial Channel Network (SCN): Opportunities and Challenges of Introducing Spatial Bypass Toward the Massive SDM Era [Invited]

Masahiko Jinno

***Abstract*—Considering middle-term predictions of the need for commercial 10-Tb/s optical interfaces working in 1-P b/s optical transport systems by 2024 and recalling the introduction of the optical bypass when entering the wavelength-abundant era in the early 2000s, we re-evaluate the values of hierarchical optical network architecture in light of the forthcoming massive spatial division multiplexing (SDM) era. We introduce a spatial channel (SCh) network (SCN) architecture, where the SDM layer is explicitly defined as a new networking layer that supports the new multiplexing technology of SDM. In an SCN, optical channels (OChs) accommodated in an express SCh bypass the overlying wavelength cross-connects (WXCs) using spatial cross-connects (SXCs) on the route. As one challenge that SCNs will present, we point out that an excessively large SXC insertion loss reduces the optical reach for spectrally groomed OChs. We show that the optical reach of spectrally groomed OChs can be maintained at almost the same level as that for an OCh transported through a conventional single-layer WDM network thanks to the low-loss features of commercially available spatial switches and foreseeable low-loss SDM multiplexers and demultiplexers. As another challenge, we discuss how to achieve growable, reliable, and cost-effective SXCs. We propose two SXC architectures based on sub-matrix switches and core-selective switches. Simple cost assessment shows that the proposed architectures are more cost-effective than the full-size matrix switch-based architecture with 1 + 1 equipment protection and conventional stacked WXC architecture.**

***Index Terms*—Core-selective switch; Matrix switch; Optical network; Spatial bypass; Spatial channel; Spatial cross-connect; Spatial division multiplexing; Wavelength division multiplexing.**

I. Introduction

In the past 10 years, research has focused on exploring space as the only remaining physical dimension for signal multiplexing to deal with the ever-increasing demand for transmission capacity in optical networks. This is because we expect to reach the fundamental capacity limits of conventional single-mode fibers (SMFs), i.e., the so-called nonlinear Shannon limit, in the near future [1]. A near-term and straightforward solution would be to use existing parallel SMFs or multiple co-packaged SMFs. As middle- or long-term solutions, a wide variety of fibers of new structures that support multiple guided spatial modes in a fiber are developing worldwide. Now we are about to enter a new era of space division multiplexing (SDM). A multicore fiber (MCF) is one such SDM fiber in which multiple single-mode cores are placed within a single fiber cladding. In general, MCFs are carefully designed to suppress the crosstalk between cores below the level allowed by the transmission system. A few-mode fiber (FMF) is another type of SDM fiber in which the core dimension is modified to support more guided spatial modes. In a FMF, guided spatial modes spatially overlap and strongly couple each other as they propagate the fiber. These intermingled modes should be routed together end to end to be untangled at the receiver using multi-input multi-output (MIMO) digital signal processing (DSP). A few-mode multicore fiber (FM-MCF) is the combination of the above fiber structures where multiple few-mode cores are placed within a single fiber cladding.

Although SDM fiber technology significantly scales in spatial mode counts S per link and network capacity, it presents a challenge in that it necessitates the deployment of large size reconfigurable optical add drop multiplexers (ROADMs) comprising a large number ($= 2DS$) of high port count ($\geq DS$) wavelength-selective switches (WSSs), where D is the node degree. In order to deal with this problem, researchers are focusing on developing scalable wavelength division multiplexing (WDM)/SDM ROADM architectures supporting a large number of SMFs or SDM fibers [2–11]. The ideas behind their approaches are based on introducing connection constraints considering the fact that all spatial modes in an SDM fiber are directed to the same adjacent node. This leads to employing less complicated and consequently cost-effective optical switches. Feuer *et al*. proposed the concept of a *spatial superchannel* and *joint switching* of spatial superchannels [3,4]. Spatial superchannels are high-rate data streams transported as groups of subchannels occupying the same frequency slot in separate modes/cores. They showed 1×2 joint switching of a spatial superchannel comprising seven spatial subchannels using seven-core MCFs interfaced with mode demultiplexers to a commercial 21-port count

Manuscript received August 20, 2018; revised November 26, 2018; accepted November 28, 2018; published January 25, 2019 (Doc. ID 335910).

The author is with the Faculty of Engineering and Design, Kagawa University, Takamatsu 761-0396, Japan (jinno@eng.kagawa-u.ac.jp).

https://doi.org/10.1364/JOCN.11.000001

Glossary

AC	Any-core access
ASE	Amplified spontaneous emission
B&S	Broadcast and select
BV-WSS	Bandwidth-variable WSS
CAGR	Compound annual growth rate
CL	Contentionless
CSS	Core-selective switch
DCI	Data-center interconnect
DL	Directionless
DP	Dual-polarization
EON	Elastic optical network
FM-MCF	Few-mode multicore fiber
FMF	Few-mode fiber
GN	Gaussian noise
HOXC	Hierarchical optical cross-connect
LC	Lane change
LR	Linear repeater
MCF	Multicore fiber
MS	Matrix switch
NLI	Nonlinear interference
OCh	Optical channel
ODU	Optical channel data unit
OR	Optical reach
OSNR	Optical signal-to-noise ratio
PSD	Power spectral density
P2P	Point to point
QAM	Quadrature amplitude modulation
R&S	Route and select
ROADM	Reconfigurable optical add drop multiplexer
SCh	Spatial channel
SCN	Spatial channel network
SDEMUX	Spatial demultiplexer
SDM	Space division multiplexing
SL	Spatial lane
SMF	Single-mode fiber
SMUX	Spatial multiplexer
SXC	Spatial cross-connect
WC	Wavelength conversion
WDEMUX	Wavelength demultiplexer
WDM	Wavelength division multiplexing
WMUX	Wavelength multiplexer
WSS	Wavelength-selective switch
WXC	Wavelength cross-connect

WSS. Fontaine *et al*. reported a joint switch for six spatial modes to eight outputs using a new type of joint-switch WSS that arranges the SMF ports in a two-dimensional array [5]. We proposed a unified architecture of an integrated SDM-WSS employing a spatial beam transformer array for various types of SDM fibers [6] and demonstrated the feasibility of integrated fractional joint switching WSS by building a 1×2 WSS prototype applicable for a FM-MCF having three cores that support two spatial modes [7]. Spectrally and spatially flexible optical networking architectures that support the joint switching of spatial superchannels were discussed in Refs. [12] and [13]. Sato *et al*. took another approach. Instead of creating a high-port-count ROADM using a large number of cascaded conventional WSSs or ultra-high-port count WSSs, they introduced a subsystem-modular wavelength cross-connect (WXC) architecture, in which multiple small-scale WXC subsystems (sub-WXCs) are connected via a limited number of intra-node SMFs. The total WXC port count can be simply expanded by adding sub-WXCs [8,9]. Recently, Nagoya University and Nippon Telegraph and Telephone (NTT) reported a subsystem-modular WXC based on an integrated 6×6 WSS that was fabricated using spatial and planar optical circuit (SPOC) technology [10,11].

It should be noted that although the joint-switching ROADMs and subsystem-modular WXCs can support SDM fibers, they are designed to be used in single-layer WDM networks. This means that as long as they handle traffic demands only in the fine granular WDM layer, they will most likely be less cost-effective in the forthcoming massive SDM era. For example, a joint-switching ROADM that supports S spatial modes per link requires high-port-count WSSs with S times the port count of that of a conventional WSS. A subsystem-modular WXC that supports S spatial modes per link requires a large number of conventional WSSs, which is S times the number of that needed in a conventional WXC. Historically speaking, a new signal multiplexing technology has needed a new networking layer and hence a new switching technology with the same switching granularity as the multiplexing granularity of the new layer. In the same way that the introduction of WDM required ROADMs/WXCs, SDM will need spatial cross-connects (SXCs) to achieve a cost-effective SDM layer. This implies that the current optical layer should evolve to hierarchical SDM and WDM layers. Hereafter, we refer to an optical network for the SDM layer as a spatial channel network (SCN). Here, an important question is when the SDM layer will yield technological and economic validity. As we show in the next section, according to the middle-term prediction of router interface speed and optical transport system capacity trends, it may happen in the not-too-distant future.

In this paper, recalling the introduction of the optical bypass when entering the wavelength abundant era in the early 2000s, we reevaluate values of the hierarchical optical network architecture and investigate a growable and reliable optical node architecture for the forthcoming massive SDM era when optical transmission lines (for example, parallel SMFs and/or MCFs) are abundant between adjacent optical nodes. The remaining part of this paper is organized as follows. In Section II, we discuss opportunities for introducing an SCN from the viewpoints of the history of optical network evolution and the trend in client-interface speed. In Section III, we define a spatial channel (SCh) in the SDM layer and present an SCN architecture, where optical channels (OChs) accommodated in an express SCh bypass the overlying WXCs by using SXCs on the route. In Section IV, we discuss challenges that SCNs present: how to balance the transmission performance, growability, reliability, and cost in an SXC design. We propose two different SXC architectures based on sub-matrix switches (sub-MSs) and core-selective switches (CSSs) and assess the architectures from optical reach, growability, reliability, and techno-economic viewpoints. In Section V,

we present our conclusions and give some remarks on future work.

II. Opportunities for Spatial Channel Networks

A. Optical Network Evolution

Let us first look back on the history of optical network evolution from the viewpoints of multiplexing technology and corresponding optical node architecture.

1) Early Optical Fiber Transmission Systems: Since optical fiber transmission systems were introduced to telecommunication networks in the early 1980s, the synchronous digital hierarchy (SDH) has been commonly used as the interface to the optical layer, where services such as the asynchronous transfer mode (ATM) and Internet protocol (IP) are assigned to time slots in SDH frames. In addition to the framing, SDH is used for time-division multiplexing (TDM) of lower-order frames into a higher-order larger frame and electrical switching of lower-order frames through an SDH cross-connect (XC) as shown in Fig. 1(a).

2) WDM and Optical Bypass: The earliest WDM systems were deployed at the beginning of the 2000s, and the number of WDM channels that were multiplexed into a fiber in the spectral domain has rapidly increased up to ~100. The optical transport network (OTN) standard has superseded SDH as the interface to the optical layer. Rapid growth in the WDM capacity has necessitated the deployment of a tremendous amount of electrical terminating and switching equipment, such as optical transponders and optical channel data unit cross-connects (ODU-XCs) or IP routers [Fig. 1(b)], where all network traffic entering the node is processed in the electrical domain. This incurs serious cost and power-consumption problems. Optical bypass technology based on optical switches has developed in order to reduce the burden of ODU-XCs or IP routers [14–16]. Nowadays, the most popular transport network architecture is the hierarchical IP (over ODU-XC) over the WDM network that comprises IP routers (and ODU-XCs) and ROADMs as shown in Fig. 1(c). In such a network, an OCh is established between a source/destination pair where a sufficient amount of traffic to fill almost the entire capacity of the wavelength exists, and the OCh bypasses the overlying OTN or IP layers in the optical domain.

3) EON and Flexible Grooming in the Optical Layer: The introduction of WDM technology dramatically reduced the network cost and propelled the spread of broadband services. However, along with the penetration and the continuous increase in speed of broadband services, revenue growth of network operators gradually plateaued. In the late 2000s, operator efforts were focused on enhancing network efficiency in order to fully utilize their existing fiber infrastructure by introducing elasticity and adaptation into WDM networks. Hereafter, we refer to such a WDM network as an elastic optical network (EON) [17–19] [Fig. 1(d)].

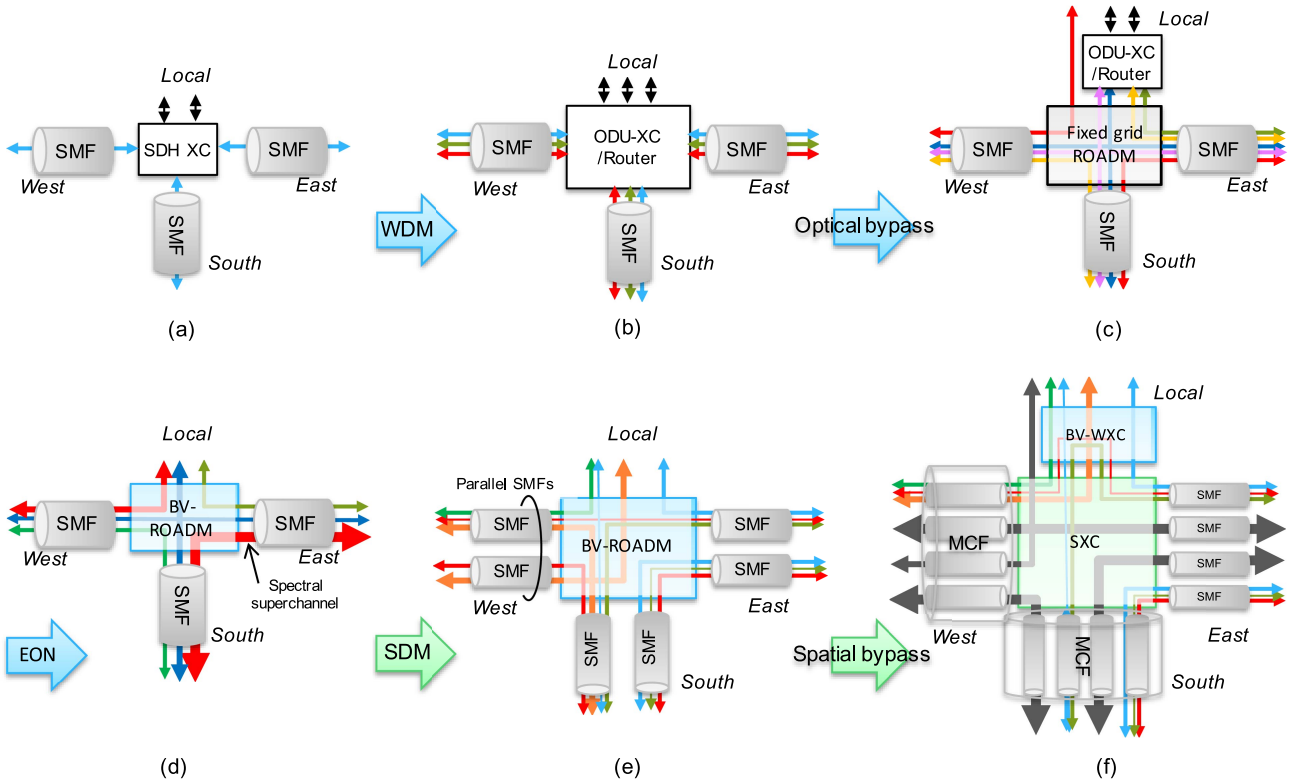

Fig. 1. Multiplexing technology and optical network evolution: past, current, and foreseeable future. (a) TDM and SDH-XC, (b) WDM and ODU-XC/IP-router, (c) optical bypass using fixed-grid ROADM, (d) optical grooming using BV-ROADM, (e) SDM and large size BV-ROADM, (f) spatial bypass using SXC.

Thanks to two evolutional technologies, digital coherent transmission technology with its associated sophisticated modulation schemes and DSP, and bandwidth-variable WSSs (BV-WSSs) based on a liquid crystal on silicon (LCoS) spatial light modulator [20], EONs can accommodate a wide variety of OChs in terms of spectral width and transmission distance and optically route OChs in a highly spectrally efficient manner. This will make the role of electrical grooming less significant for high-capacity OChs with bit rates higher than 100 Gb/s, thus achieving cost-effective and low-power-consuming WDM networks.

4) Current Research Trend for Adopting SDM: In the same way as when WDM technology was introduced to optical networks, currently in progress advances in SDM technology present a challenge in that they necessitate the deployment of large ROADMs with tremendous numbers of conventional WSSs. In order to deal with this problem, researchers are focusing on developing scalable WDM/SDM ROADM/WXC architectures supporting a large number of SMFs or SDM fibers such as MCFs, as shown in Fig. 1(e), through the introduction of reasonable connection constraints and integration into ROADM/WXC architectures. Recently, joint switching of a spatial superchannel based on an ultra-high port count ROADM, where a single switching element is shared among constituting spatial sub-channels [3–7] and a subsystem-modular WXC architecture in which multiple small-scale sub-WXCs are connected via a limited number of intra-node SMFs, were also proposed [8–11]. It should be noted that, although the joint-switching ROADMs and subsystem-modular WXCs can support SDM fibers, they are designed to be used in single-layer WDM networks.

B. Opportunity for Spatial Bypass in Massive SDM Era

If we compare Figs. 1(b) and 1(e) and recall the introduction of an "optical bypass" when entering the wavelength abundant era in the early 2000s, it would be natural to consider introducing a "spatial bypass" through an SXC rather than working on achieving larger scale single-layer ROADM/WXCs in the forthcoming massive SDM era as shown in Fig. 1(f). Based on Figs. 1(a)–1(f), we realize that a new multiplexing technology should come with a new networking layer and a switching technology with the same switching granularity as the multiplexing granularity of the layer. In the same way as TDM requires SDH/ODU-XCs or IP routers and WDM requires ROADMs/WXCs, SDM will need SXCs to achieve a cost-effective SDM layer.

As a matter of fact, the idea of hierarchical (or multi-granular) optical networks, in which coarser granular but a more cost-effective switching layer(s) than the wavelength layer is introduced, is not new at all. The concept of coarser granular optical switching in the wavelength band and fiber layers was already proposed at the end of the 1990s [21–23]. Since then, there have been considerable research efforts [24,25]; however, they have remained rather notional even after SDM technology began to gather much attention [26–28] and, to the best of our knowledge, there are no reports that have focused on practical issues such as the growability, reliability, and techno-economics of hierarchical optical node architectures. One reason for this is because the idea of waveband routing was superseded by the more flexible spectral superchannel routing using BV-WSSs in EONs. Another possible reason is because fiber switching has been considered unrealistic in the past and current WDM eras, when the spectral width that an OCh occupies (for example, 50 GHz) is far less than the entire available spectrum of an SMF.

Now, an important question is when will the SDM layer yield technological and economic validity. In the next subsection, we show that this may happen in the not-too-distant future.

C. Client Interface Speed Approaching Fiber Available Bandwidth

Winzer *et al.* recently reported that the recent compound annual growth rates (CAGRs) of the aggregate router blade interface rate are at approximately 40% and predicted the need for commercial 10-Tb/s optical interfaces working in 1-P b/s optical transport systems by 2024 in order to accommodate such rapidly increasing client interface speeds [29]. They also reported that single-carrier optical interfaces used in commercial optical transport systems have shown a lower CAGR of 20% since the mid 1980s, limited by the scaling of cost-effective high-speed electronics and optoelectronics. The state-of-the-art commercial WDM systems operate at single-carrier bit rates as high as 400 Gb/s, and sustaining this 20% scaling has been mainly achieved through the use of polarization-division multiplexing and higher-order quadrature amplitude modulation (QAM). On the other hand, recent per-year increases in symbol rates are even lower, at approximately 10%. According to these observations and the extrapolation of trends in single-carrier optical line interface rates starting at 2010, we expect that by 2024 the single-carrier bit rate will reach 1 Tb/s, most likely by employing ~100 GBaud dual-polarization (DP) 64QAM. Although higher-order QAM provides higher spectral efficiency, it involves a considerable reduction in the optical reach. For this reason, a 10-Tb/s optical interface that is predicted to be needed by 2024 will be implemented using various combinations of the bits per symbol and the number of subchannels. For example, ten 107-GBaud DP-64QAM subchannels, twenty-five 64-GBaud DP-16QAM subchannels, or one hundred 32-GBaud DP-QPSK subchannels will be selected according to the required transmission distance.

Figure 2 shows the number of spectral superchannels that can be accommodated in a 4.4-THz spectral range (C band) as a function of the capacity of a spectral superchannel employing 32-GBaud DP-QPSK, 64-GBaud DP-16QAM, and 107-GBaud DP-64QAM, respectively. Here, we assumed the International Telecommunication Union Telecommunication Standardization Sector (ITU-T) G.694.1 flexible grid and zero-roll-off Nyquist WDM

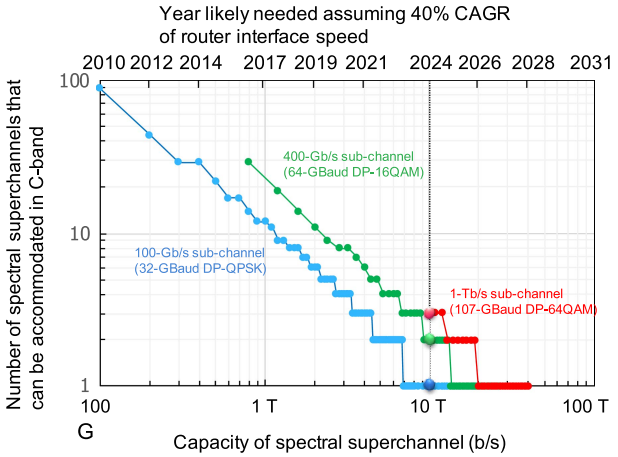

Fig. 2. Accommodatable number of spectral superchannels in the C-band.

superchannels with a reasonable guard band between superchannels. The scale on the horizontal axis on the upper part of the graph shows the year expected to require the capacity of the spectral superchannel shown on the lower horizontal axis assuming the CAGR of 40%. Since a 10-Tb/s DP-QPSK superchannel occupies at least 3.2 THz, conventional SMFs can accommodate only a single OCh in the C band by 2023. Of course, we can employ three-fold spectrally efficient DP-64QAM at the expense of an extremely shorter optical reach; however, we only gain a few additional years before a spectral superchannel will occupy the entire C band. It is quite clear that for such an ultra-high-capacity superchannel, the wavelength switching layer is no longer necessary, as suggested in Ref. [29]. Since the foreseeable 1-P b/s optical transport system capacity in 2024 far exceeds the conventional SMF capacity limit, there will be massive parallel SMFs (for example, a few dozens to ~100) and/or MCFs between adjacent optical nodes.

III. Definition of a Spatial Channel Network

In the forthcoming massive SDM era when, as mentioned in the previous section, optical transport networks comprise parallel SMF/MCF links and support ultra-high-capacity OChs whose spectral widths are compatible with or even wider than the available spectral widths of a single-mode core in an SMF or an MCF, we believe an SCN architecture would be a cost-effective and realistic solution. Figure 3 shows an SCN architecture [30]. In the SDM layer, the architecture comprises spatial SDM links and SXCs. An SDM link comprises multiple "spatial lanes" (SLs), whose physical entities are single-mode cores in parallel SMFs or/and parallel MCFs. Of course, there exist other SDM fiber technologies such as FMFs, coupled-core MCFs, and FM-MCFs. However, we do not include them in our discussion and leave the application of these SDM fibers to SCNs as a future research subject, since they are less compatible with the conventional SMF technology in terms of requiring a complicated MIMO DSP for the spatial demultiplexing and may need a longer time to be widely deployed, at least in terrestrial systems. An SXC serves as the main switch at a hierarchical optical XC (HOXC). In the WDM layer, a wavelength multiplexer/demultiplexer (WMUX/WDEMUX) and a WXC perform wavelength-level multiplexing and grooming. A WXC serves as an edge switch at an HOXC.

As high-capacity OChs, spectral superchannels [17,31] and spatial superchannels [3] have been proposed so far. A spectral superchannel is defined as a data stream that is transported as a group of subchannels that are densely aligned adjacent to each other in the frequency domain in the same core. A spatial superchannel is defined as a data stream that is transported as a group of subchannels

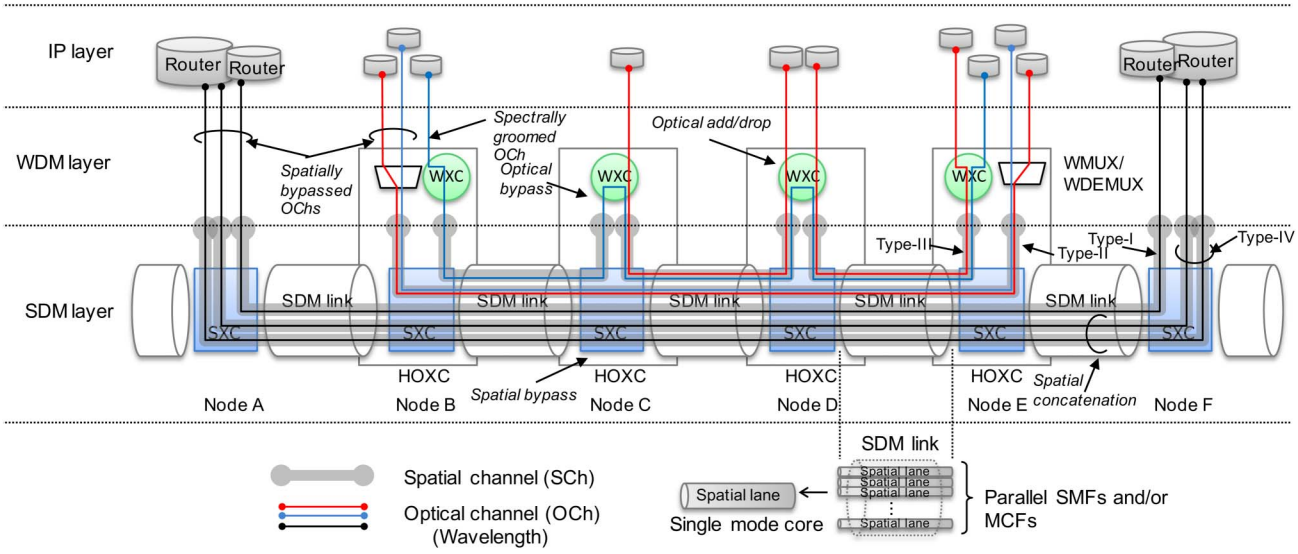

Fig. 3. Spatial channel network (SCN) model.

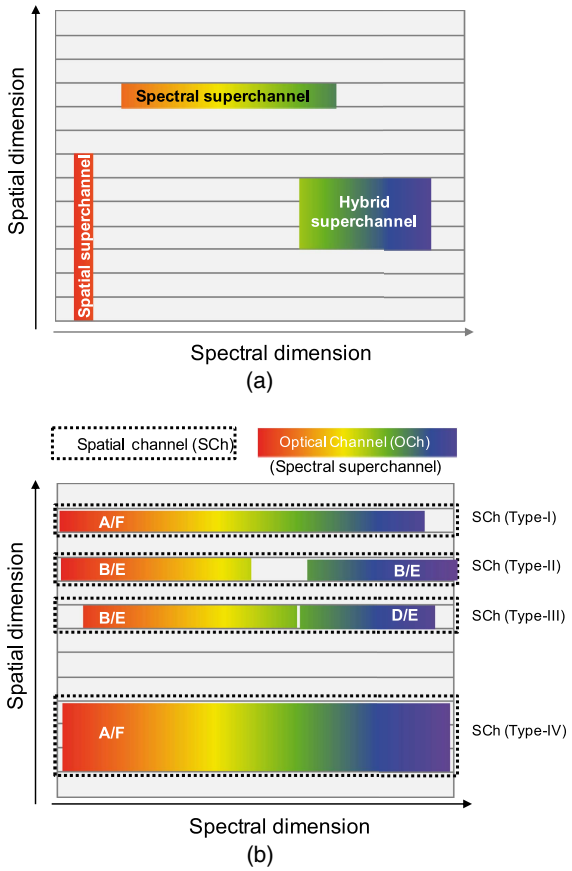

Fig. 4. Spectral-superchannel, spatial-superchannel, and spatial channel examples. Each OCh in an SCh is labeled with names of the source/destination node pairs. (a) Spectral and spatial superchannels and (b) spatial channels (SCh).

occupying the same frequency slot in separate cores. Examples of spectral and spatial superchannels in the spectral-spatial plane are shown in Fig. 4(a) together with a hybrid superchannel, which is a concept that combines them [29].

In an SCN, we define an SCh as an ultra-high-capacity optical data stream that is allowed to occupy the entire available spectrum of, for example, a core in an SMF or an MCF [See Fig. 4(b)] and is optically routed end to end as a single entity through SXCs bypassing the overlying WDM layer. In comparison to spatial superchannels, spectral superchannels have advantages in terms of higher compatibility with current WDM technology, no need for parallel fibers at the initial stage, higher spectral efficiency, and reduced penalties from optical filter concatenation [29]. SChs inherit the advantages of spectral superchannels; moreover, SChs achieve the highest spectral efficiency and do not suffer filter penalties at all thanks to the spatial bypassing of the overlying WDM layer.

An SCh transports a single or multiple OChs that is (are) spectrally aligned with the G.694.1 flexible grid paradigm. There are four types of SChs according to the OChs they carry:

- Type I: an SCh carrying a single large-capacity OCh,
- Type II: an SCh carrying multiple OChs with the same source/destination node pair,
- Type III: an SCh carrying multiple OChs with different source/destination node pairs,
- Type IV: an SCh comprising concatenated SChs to carry an OCh with a capacity higher than that of an SCh.

If there is a single or aggregate traffic flow that is sufficiently large to fill almost the entire bandwidth of an SCh between the source and destination nodes, an SCh is established between them [see Type-I and Type-II SChs in Figs. 3 and 4(b)]. Such SChs bypass the overlying WDM layer (spatial bypass). Thanks to the low-cost coarse granular switching characteristics of spatial switches, they enjoy a lower switching cost per bit as discussed in Section IV.B. Here, OChs in an SCh of Type I or Type II are described as "spatially bypassed." If there is an insufficient amount of traffic between a source/destination pair, the corresponding OCh shares an SCh (Type III) with other low-capacity OChs having different source/destination pairs for a better utilization of spatial resources. SChs carrying such low-capacity OChs, which are either destined for the site (optical drop) or being further groomed (optical bypass) in the WDM layer by a ROADM/WXC at the site, are dropped by the SXC (SCh drop). The latter OChs are described as "spectrally groomed." In this way, only the necessary minimum number of ROADMs/WXCs is deployed in a SCN. On the other hand, an OCh with a capacity higher than that of an SCh is inverse-multiplexed to multiple concatenated SChs (Type IV, spatial concatenation). The capacity of a concatenated SCh can be varied according to the traffic demand by changing the number of cores that is assigned to the concatenated SCh. In this way, the HOXC architecture can support a wide variety of traffic demands from 100 Gb/s to 10 Tb/s or even higher.

IV. Challenges and Directions for Spatial Channel Networks

In this section, we first discuss the challenges that SCNs present: how to balance the transmission performance, growability, reliability, and cost in an SXC design. The following two sub-sections provide directions for addressing the challenges: analytical results for an allowable SXC loss and proposals for growable and reliable SXC architectures.

A. Challenges That SCNs Present

A mandatory requirement for SXCs from the viewpoint of physical performance is that the insertion loss of SXCs must be sufficiently low so that it does not degrade the transmission performance of spectrally groomed OChs. Since spectrally groomed OChs pass through the SXC twice (drop and add) at every grooming site in the WDM layer, they accumulate more amplified spontaneous emission (ASE) noise generated by optical amplifiers used for compensating for the insertion loss of an SXC than those

accumulated by OChs in conventional single-layer WDM networks. The greater the SXC insertion loss, the shorter the optical reach (OR) of a spectrally groomed OCh becomes due to greater amounts of accumulated ASE noise. The major components of an SXC are a spatial multiplexer/demultiplexer (SMUX/SDEMUX) and a spatial switch in the form of $N \times N$ or $1 \times N$. Since an excessively large OR reduction in spectrally groomed OChs may diminish the value of introducing the SCN architecture, reducing the losses of SXCs is of significant importance.

From an operational point of view, a mandatory requirement for SXCs is reliability based on the design policy to ensure that there is no single point of failure or small failure group. The growability in terms of the node degree (2 to 8), add-drop ratio (up to 50%), and number of SLs that ensure a low start-up cost and pay-as-you-grow approach is generally mandatory and especially favored in terrestrial systems. Therefore, we need to develop reliable and growable SXC architectures in a cost-effective manner. As for the connection flexibility of an SXC, fully non-blocking connectivity for an SCh in an SXC can be expressed as "any core (spatial lane) from any direction (SDM link) can be connected to any transceiver or any core of any direction". According to the terminology used in current ROADMs, colorless, directionless, and contentionless features and the wavelength conversion (WC) capability, the full connectivity for an SCh can be decomposed into some degrees of connection freedom. We refer to these as any-core access (AC), directionless (DL), contentionless (CL) features and a lane-change (LC) capability, respectively. Since they are associated with additional cost, different network operators or over-the-top (OTT) players may have different preferences.

B. GN Model Analysis for Allowable SXC Loss

We investigated ORs for a spatially bypassed OCh and a spectrally groomed OCh based on Gaussian noise (GN) model analysis in dispersion-uncompensated fiber links [32,33] as a function of SXC loss β_s. The SCN and HOXC models used in the calculation are shown in Fig. 5(a). The SCN model comprises a HOXC, SDM linear repeaters [LRs, not shown in Fig. 5(a)], and SDM links having the same length L and the same transmission loss α, which is compensated for 100% by an LR. An SXC is placed every n SDM links. The HOXC model comprises an SXC, a WXC with loss β_w of 20 dB, and optical amplifiers that compensate for the transmission loss α of the SDM link, insertion loss β_s of the SXC, and insertion loss β_w of the WXC. If we assume the per kilometer fiber loss of 0.25 dB/km, span lengths L of 40, 60, and 80 km yield span losses $\alpha = 10$, 15, and 20 dB, respectively.

In dispersion-uncompensated SMF links, nonlinearity acts as additive GN, which is referred to as nonlinear interference (NLI) [32,33]. At the end of a multi-span transmission system, the power spectral density (PSD) of the NLI produced in a span is simply added to those produced in all others to obtain the total PSD of the NLI in the same manner as ASE noise generated from an optical amplifier placed in every fiber span. If we assume that OChs have a

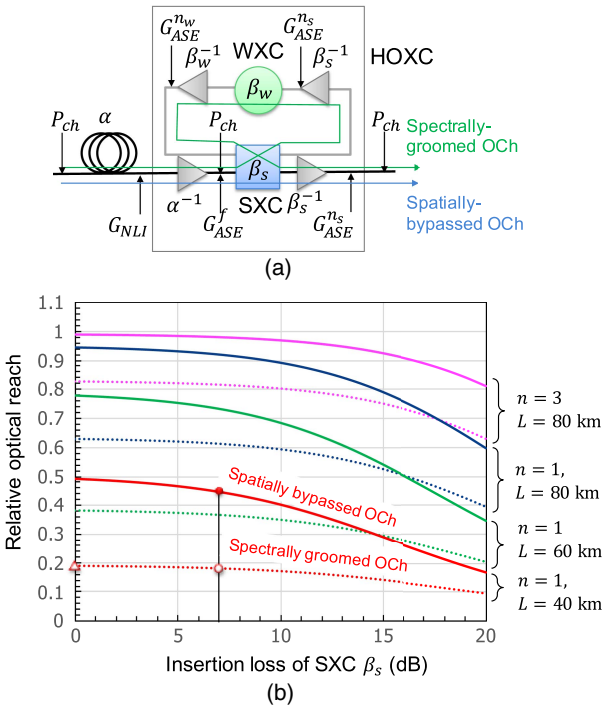

Fig. 5. Relative optical reach for spatially bypassed and spectrally groomed OChs as functions of SXC insertion loss. (a) SCN and HOXC models and (b) calculation results of relative optical reach.

rectangular spectrum with a bandwidth equal to symbol rate R, have a uniform height signal PSD (G_{WDM}), and are aligned with a frequency spacing equal to the symbol rate (Nyquist limit) over the full available optical band, the optical signal-to-noise ratio (OSNR) for an OCh defined by the ratio of the signal power P_{ch} to the ASE and NLI noise powers $P_{\mathrm{ASE}} + P_{\mathrm{NLI}}$ is given by [32,33]

$$\mathrm{OSNR}_{\mathrm{ASE,NLI}} = \frac{P_{\mathrm{ch}}}{P_{\mathrm{ASE}} + P_{\mathrm{NLI}}} = \frac{G_{\mathrm{WDM}}}{a + bG_{\mathrm{WDM}}^3}, \tag{1}$$

where a is the factor relating to the ASE noise and depends on losses that an OCh experiences along the route. ASE noise factors for the OCh in a conventional point-to-point (P2P) system a_p, spatially bypassed OCh a_b, and spectrally groomed OCh a_g, are given by

$$a_p = \frac{B_{\mathrm{ref}} N_f h\nu F}{R}\left(\frac{1}{\alpha} - 1\right), \tag{2a}$$

$$a_b = \frac{B_{\mathrm{ref}} N_f h\nu F}{R}\left\{\left(\frac{1}{\alpha} - 1\right) + \left(\frac{1}{\beta_s} - 1\right)\frac{1}{n}\right\}, \tag{2b}$$

$$a_g = \frac{B_{\mathrm{ref}} N_f h\nu F}{R}\left\{\left(\frac{1}{\alpha} - 1\right) + \left(\frac{2}{\beta_s} + \frac{1}{\beta_w} - 3\right)\frac{1}{n}\right\}, \tag{2c}$$

respectively, where B_{ref} is an optical reference bandwidth, N_f is the number of fiber spans, h is Planck's constant, ν is the center optical frequency of the OCh, and F is the noise figure of the amplifier [34]. Factor b is related to the NLI noise and given by

$$b = \frac{B_{\text{ref}} N_f}{R\alpha}\rho, \tag{3}$$

where ρ is the NLI coefficient of the fiber.

The maximum OSNR available at the optimum launched signal PSD is given by

$$\text{OSNR}_{\text{ASE,NLI}}|_{\max} = \frac{1}{3}\left(\frac{4}{a^2 b}\right)^{\frac{1}{3}}. \tag{4}$$

It should be noted that if the height of launched signal PSD is optimal for the spectrally groomed OCh, it is suboptimal for the spatially bypassed OCh, and vice versa. The resulting suboptimal OSNRs for the spatially bypassed OCh is given by

$$\text{OSNR}^{\text{bypass}}_{\text{ASE,NLI}}|_{\text{suboptimal}} = \frac{1}{a_g + 2a_b}\left(\frac{4a_g}{b}\right)^{\frac{1}{3}}. \tag{5}$$

Since the maximum and suboptimal OSNRs are simply inversely proportional to the number of fiber spans, N_f, if the required OSNR at the receiver is given, the OR can be derived by solving Eqs. (1)–(5) for N_f. The optical reach for a spectrally groomed OCh in an SCN normalized by that for an OCh in a P2P system is given by

$$\frac{N_f^{\text{groom}}|_{\max}}{N_f^{p2p}|_{\max}} = \left[\frac{\frac{1}{\alpha}-1}{\left(\frac{1}{\alpha}-1\right)+\left(\frac{2}{\beta_s}+\frac{1}{\beta_w}-3\right)\frac{1}{n}}\right]^{\frac{2}{3}}, \tag{6}$$

where the height of launched signal PSD is optimal for the spectrally groomed OCh. This signal launching condition yields a suboptimal optical reach for a spatially bypassed OCh as

$$\frac{N_f^{\text{bypass}}|_{\text{suboptimal}}}{N_f^{P2P}|_{\max}} = \frac{3\left(\frac{1}{\alpha}-1\right)^{\frac{2}{3}}\left\{\left(\frac{1}{\alpha}-1\right)+\left(\frac{2}{\beta_s}+\frac{1}{\beta_w}-3\right)\frac{1}{n}\right\}^{\frac{1}{3}}}{\left\{\left(\frac{1}{\alpha}-1\right)+\left(\frac{2}{\beta_s}+\frac{1}{\beta_w}-3\right)\frac{1}{n}\right\}+2\left\{\left(\frac{1}{\alpha}-1\right)+\left(\frac{1}{\beta_s}-1\right)\frac{1}{n}\right\}}. \tag{7}$$

Figure 5(b) shows the relative OR as a function of SXC loss for a spatially bypassed OCh (solid lines) and a spectrally groomed OCh (dotted lines) normalized by that for an OCh in a P2P system, when the launched signal power is optimized for a spectrally groomed OCh that experiences additional SXC and WXC losses resulting in a suboptimal OR for a spatially bypassed OCh. When SXC insertion loss $\beta_s = 1$, the relative OR for a spectrally groomed OCh corresponds to that for an OCh transported through a conventional single-layer WDM network. It gradually decreases as β_s increases. From Fig. 5, we can see that in order to achieve a relative OR that is almost the same level as that for an OCh transported through a conventional single-layer WDM network (for example >95%), we need an SXC with an insertion loss β_s of less than 7 dB. Fortunately, $N \times N$ and $1 \times N$ optical switches with a sufficiently low insertion loss (≤2 dB) are commercially available. On the other hand, the insertion losses of SMUXs/SDEMUXs can be much lower [35,36] than those of WMUXs/WDEMUXs. For example, for the fiber-bundle type, compact SMUXs/SDEMUXs for a seven-core MCF with the insertion loss of <0.3 dB [35] and for a 19-core MCF with the insertion loss, total crosstalk, length, and outer diameter of <1.15 dB, <−59 dB, 15 mm, and 2 mm, respectively [36], were reported. Moreover, parallel SMFs never explicitly require any SMUX/SDEMUX. Therefore, if appropriate switching technologies are selected, there would be a great possibility that well-designed SXCs will achieve an insertion loss β_s of less than 7 dB. This low-loss feature of SXCs is advantageous over conventional waveband XCs that have a relatively high insertion loss of approximately 18 dB [25].

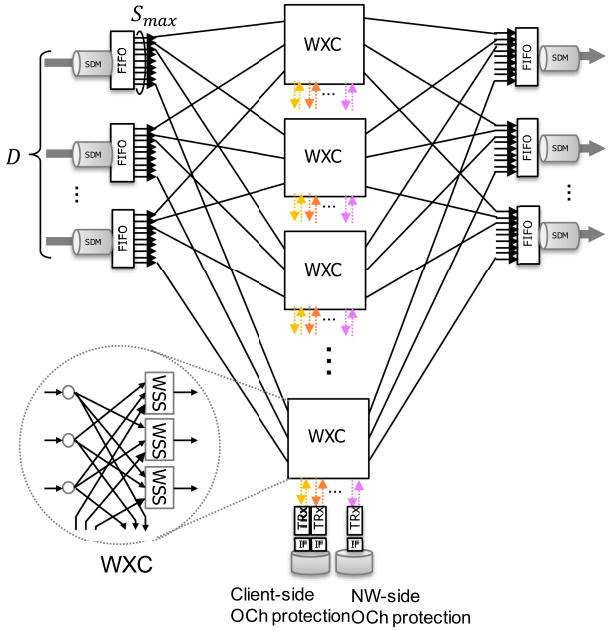

Fig. 6. Baseline stacked WXC architecture.

Such a low-loss SXC will bring added value to SCNs [30] as we can see from Fig. 5. A relative OR for the spatially bypassed OCh significantly increases from that for the OCh transported through a conventional single-layer WDM network, especially for networks with shorter span lengths such as data-center interconnects (DCIs) and metro networks, e.g., for $\alpha = 10$ dB ($L = 40$ km), $\beta_s = 7$ dB, and $n = 1$, the OR increases by 2.3-fold.

C. Growable and Reliable SXC Architectures and Cost Assessment

1) Baseline Stacked WXC Architecture: Figure 6 shows the stacked conventional WXC architecture as a baseline.

Each port of a WXC is connected to an SL having the same index as the index of the WXC in each SDM link with S SLs, where S is the number of SLs per link. This results in S stacked *single-layer* WDM networks. If we use MCFs, an SMUX and SDEMUX are needed for each input and output MCF pair. Although this architecture provides dedicated core access and no LC capability for OChs, it provides fine granular spectral grooming. This architecture is growable in terms of the number of SLs. The reliability is assured by employing fault-independent client-side or network-side OCh protections in the same way as in current WDM networks (optical protection switches are not explicitly shown in the figure). However, we need a huge number of conventional WSSs. If we assume the Broadcast and Select (B&S) architecture, the directional add/drop part, and no interconnection between WXCs for simplicity, the required total number of WSSs for this baseline node architecture becomes SD, where D is the node degree. For example, if $S = 64$ and $D = 4$, we need 256 WSSs.

2) Full-Size Matrix-Switch-Based Architecture: Figure 7(a) shows a HOXC architecture that employs an SXC based on high-port-count matrix switches (MSs), which is the same as a traditional fiber XC architecture that appears in the literature. Preparing for an MS failure, a secondary high port count MS that is connected in parallel with the primary MS with optical splitters and optical 2×1 switches are implemented (equipment protection). When the primary MS fails, optical 2×1 switches that accommodate the affected SChs switch over the connection to the secondary MS. On the other hand, when a link along the working SCh fails, IP/MPLS (multiprotocol label switching) routes or MSs at the endpoints of the working SCh reroute the connection to a diverse route. The former is referred to as client-side protection and the latter as network-side SCh protection (not shown for better visibility). The advantage of this architecture is that it provides fully non-blocking connection flexibility in terms of AC, DL, CL, and LC as shown in Fig. 7(b) (only the upward paths are shown).

One disadvantage of this architecture is that it is not cost-effective and growable because double the cost of an MS with the maximum switch size expected to be necessary in the future must be paid from the very beginning. The required size of an MS is given by $\lceil S_{\max} D(1+d) \rceil \times \lceil S_{\max} D(1+d) \rceil$, where $S_{\max}$ is the maximum number of SLs per link that the system accommodates, d is the SCh add-drop ratio, and $\lceil \cdot \rceil$ is the ceiling function. In addition, for spectral grooming in the WDM layer, we need dgS conventional WXCs, where g is the spectrally groomed ratio of the added/dropped SChs. If we assume the B&S WXC architecture and the directional add/drop part for simplicity, the required total number of WSSs becomes $dgSD$. If $S_{\max} = 64$, $D = 4$, $d = 1/4$, and $g = 1/2$, we need two 320×320 MSs at the time of system deployment and eight ROADMs (32 WSSs) in total at the end of the system life.

Another disadvantage of this architecture is the mixture of fault-dependent protection mechanisms for equipment and link failures. Fault-dependent protection requires a fault localization process before a switchover action can be executed to avoid a conflict in protection mechanisms, which requires complicated negotiation between protection mechanisms and may incur a longer recovery time [37]. This means that even though the IP layer employs client-side SCh protection or IP/MPLS layer recovery, which provides protection against a router interface failure and a transponder failure in addition to protection against link failure, they are ineffective for an MS failure as long as both the working and backup paths are accommodated in a single full-size MS-based SXC. This is because a full-size MS-based SXC is not port modular and so both the working and backup paths are simultaneously blocked by the failed MS. This may diminish the advantage of fast IP/MPLS layer recovery.

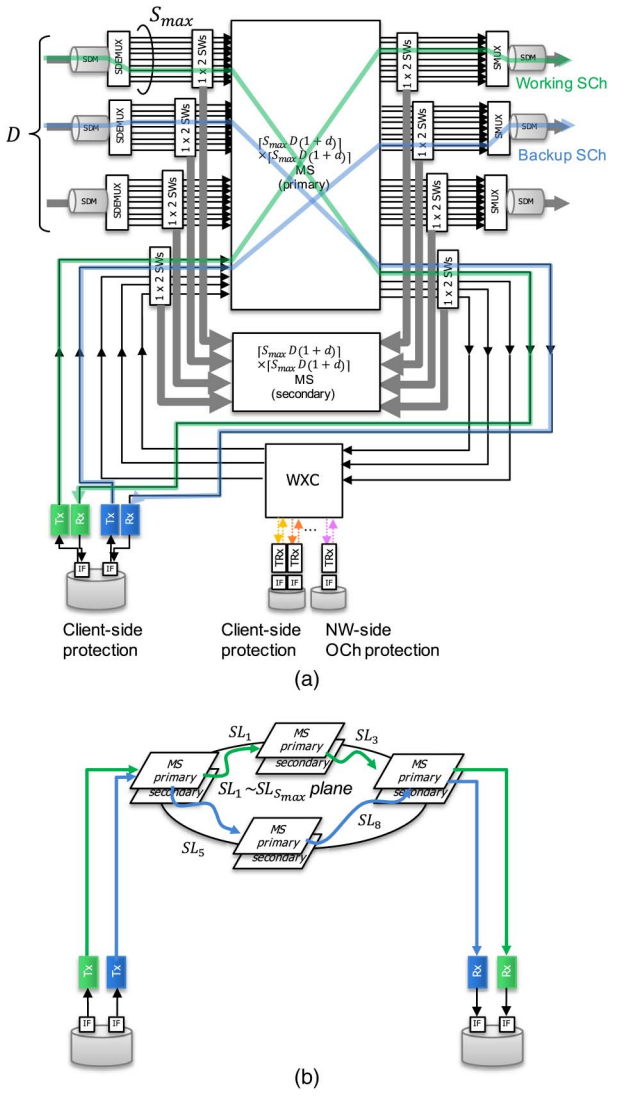

Fig. 7. HOXC architecture employing full-size MS-based SXC and SCN models. (a) HOXC architecture and (b) SCN model.

3) Sub-Matrix-Switch-Based Architecture: In order to address the above-mentioned problems in a full-size

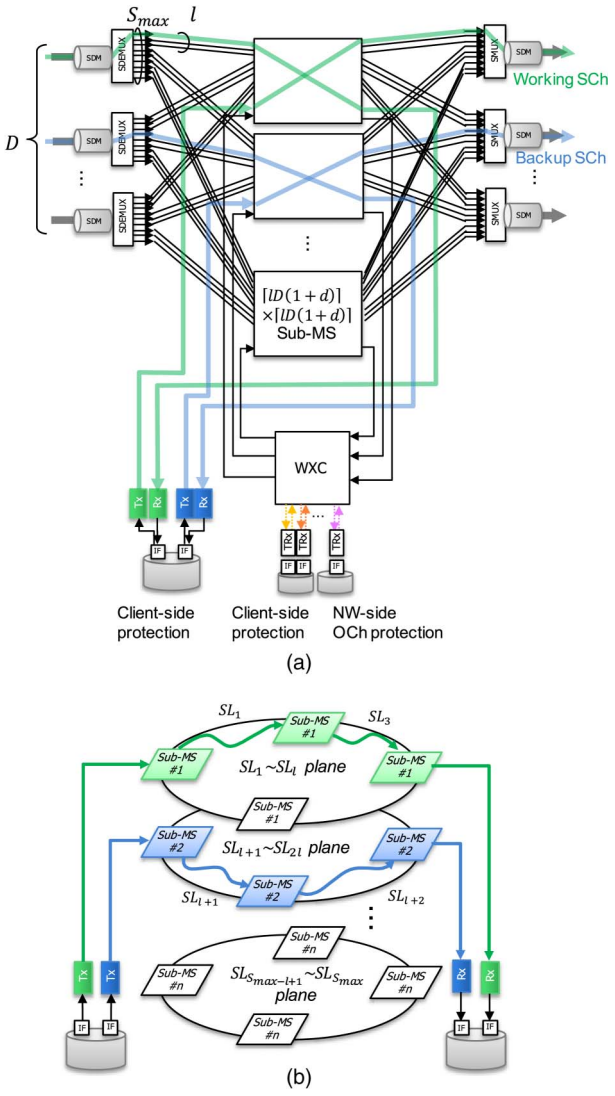

Fig. 8. HOXC architecture employing sub-MS based SXC. (a) HOXC architecture and (b) SCN model.

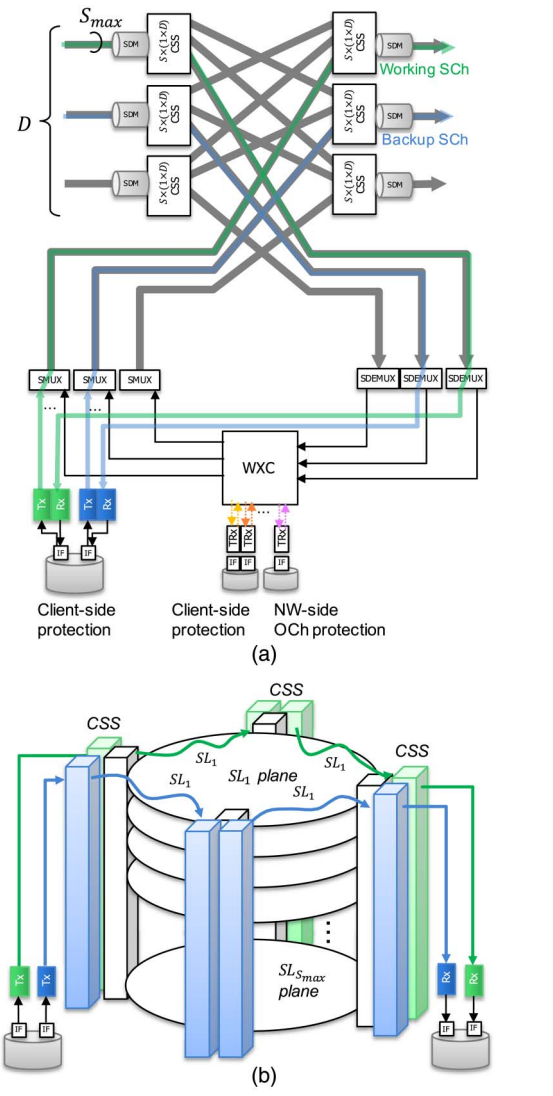

Fig. 9. HOXC architecture employing CSS based SXC. (a) HOXC architecture and (b) SCN model.

MS-based SXC, we recently proposed a novel HOXC architecture employing the sub-MS-based SXC [30] shown in Fig. 8(a). In this architecture, the $\lceil S_{\max}D(1+d) \rceil \times \lceil S_{\max}D(1+d) \rceil$ full MS in Fig. 7 is divided into $S_{\max}/l$ sub-MSs with the size of $lD(1+d) \times lD(1+d)$, where l is the number of sub-spatial lanes (sub-SLs) per each SDM link that each sub-MS accommodates. This sub-MS-based architecture ensures the growability in terms of the number of SLs and enables the fault-independent path protection as shown in Fig. 8(b) at the expense of a limitation to the connection flexibility for SChs similar to current WSS-based ROADMs and subsystem modular WXCs [7–9]. By choosing working (green line) and backup (blue line) routes to be SDM-link disjoint and sub-MS disjoint from each other, this architecture supports fault-independent client-side protection or network-side SCh protection (not shown for better visibility), which covers both an SDM link failure and a sub-MS failure without any extra switch resources for equipment protection. It should be noted that this SXC architecture can provide partial AC and partial LC among l SLs. For the same conditions mentioned above and $l = 8$, the required sub-MS count and the size become 8 and 40×40, respectively.

For spectral grooming in the WDM layer, we need $\lceil agS \rceil$ conventional WXCs each comprising D WSSs. The minimum number of sub-MSs necessary for ensuring the reliability for spectrally groomed OChs is equal to the node degree D. For such an SXC with the minimal sub-MS count $D(= \lceil S_{\max}/l \rceil)$, the required size of the sub-MS becomes $\lceil S_{\max}(1+d) \rceil \times \lceil S_{\max}(1+d) \rceil$.

4) Core-Selective-Switch-Based Architecture: Figure 9(a) shows another architecture for balancing the growability, reliability, and cost-effectiveness in SXC design based on a $1 \times n$ core-selective switch (CSS) [30]. A CSS is the SDM counterpart of a WSS in a WDM network and has functionalities of spatially demultiplexing SChs from a common SDM port and switching and multiplexing any

of them into any of n output SDM ports. A CSS that supports $S_{\max}$ SLs can be implemented using an SDEMUX, an array of $S_{\max}$ $1 \times n$ spatial switches, and n SMUXs. Free-space optics and waveguide optics may be applied to achieve CSSs. Since this SXC architecture is port modular, it supports fault-independent client-side protection or network-side SCh protection (not shown for better visibility) by choosing working (green line) and backup (blue line) routes to be SDM-link disjoint from each other as shown in Fig. 9(b) in the same way as current WDM networks. Working and backup routes can use the same SL index or a different SL index. In order to achieve low-loss SXCs, CSSs should be used in the route and select (R&S) configuration to avoid a splitting loss, which implies that we need $2D$ $1 \times D$ CSSs that support $S_{\max}$ SLs. For the same conditions mentioned above, we need eight $1 \times D$ CSSs that support 64 SLs. Again, for spectral grooming in the WDM layer, we need $\lceil dgS_{\max} \rceil$ conventional ROADMs/WXCs, each comprising D WSSs. This SXC architecture is growable in terms of the nodal degree and provides dedicated core access and no LC.

Such a full-size CSS can be divided into smaller CSSs, for example, $S_{\max}/l$ $1 \times D$ CSSs supporting l SLs, if needed. This yields additional growability of an SXC in terms of the number of SLs. Hereafter, we refer to this architecture as sub-CSS-based SXC architecture to distinguish it from one based on full-size CSSs.

5) Cost Assessments: The total cost of the baseline single-layer stacked WXC architecture C_{wss} shown in Fig. 6 is given as a function of the number of SLs per link S, by

$$C_{\text{wss}}(S) = \text{SD} \cdot c_{\text{wss}}, \tag{8}$$

where c_{wss} is the cost of a conventional 1×9 WSS. The total cost of HOXCs based on full-size MSs C_{fms}, sub-MSs C_{sms}, and full-size CSSs C_{fcss} shown in Figs. 7–9, and sub-CSSs C_{scss} (not shown) are given as a function of S by

$$C_{\text{fms}}(S) = 2 \cdot \text{c}_{\text{ms}}(\lceil S_{\max} D(1+d) \rceil) + \lceil dgS \rceil D \cdot c_{\text{wss}}, \tag{9}$$

$$C_{\text{sms}}(S) = \lceil S/l \rceil \cdot \text{c}_{\text{ms}}(\lceil lD(1+d) \rceil) + \lceil dgS \rceil D \cdot c_{\text{wss}}, \tag{10}$$

$$C_{\text{fcss}}(S) = 2D \cdot c_{\text{css}}(S_{\max}) + \lceil dgS \rceil D \cdot c_{\text{wss}}, \tag{11}$$

$$C_{\text{scss}}(S) = \lceil S/l \rceil \cdot 2D \cdot c_{\text{css}}(l) + \lceil dgS \rceil D \cdot c_{\text{wss}}, \tag{12}$$

respectively. Here, $c_{\text{ms}}(N)$ and $c_{\text{css}}(l)$ are defined as functions that give the costs of an $N \times N$ MS and l-port 1×9 CSS, respectively. Costs corresponding to an add/drop part of an SXC and WXCs are not included in these formulas since they strongly depend on how much connection flexibility is required in the SCN, and different network operators or OTT players likely have different requirements. The cost of an SMUX/SDEMUX is also not included because it is considered to be negligibly small.

According to private communications with some vendors, we assume that the cost of a 32×32 MS, c_{ms}^{32}, is 3.75 times the cost of a 1×9 WSS c_{wss} that supports 96 wavelengths in the C band. It may depend on the employed technologies used whether the cost of an $N \times N$ MS, $c_{\text{ms}}(N)$, increases with port count N sub-linearly (due to the cost reduction by sharing the costs of common devices and common production processes) or super-linearly (due to adjustment and testing costs that may increase with the square of the port count). It is also affected by the vendor pricing strategy. Considering these uncertainties, we introduce a parameter p (> 0) and assume that $c_{\text{ms}}(N)$ increases with port count N as $c_{\text{ms}}(N) = c_{\text{ms}}^{32} \cdot (N/32)^p$. If we assume $p = 1$, this means that $c_{\text{ms}}(N)$ increases linearly with port count N and eliminates the dependency of C_{sms} on the size of a sub-MS.

Although there has been no commercially available CSS yet, if one is constructed using free-space optics, it will most likely have a beam steering mechanism similar to that of a conventional WSS and an even simpler SDEMUX/SMUX part. For this reason, we expect that the cost of a 1×9 CSS that supports $40 \sim 80$ SLs is probably comparable to or less than that of a conventional 1×9 WSS supporting ~80 wavelengths ($c_{\text{css}}/c_{\text{wss}} \leq 1$) and decreases with the number of SLs l. Considering these expectations, we use the cost model of a CSS that supports l SLs, $c_{\text{css}}(l) = c_{\text{css}}^{64} \cdot \{(1-q)l + 64q - 1\}/63$, where c_{css}^{64} is the cost of a CSS supporting 64 SLs, and q (≤ 1) is a parameter that gives the cost of a CSS when $l = 1$. If we assume $q = 1$, this means that c_{css} is independent of the supportable number of SLs l and equal to c_{css}^{64} for all values of l. On the other hand, when $q = 1/64$, $c_{\text{css}}(l)$ is simply given by $c_{\text{css}}^{64} \cdot (l/64)$.

Figure 10 shows the total costs of the above-mentioned four HOXC architectures given by Eqs. (9)–(12) together

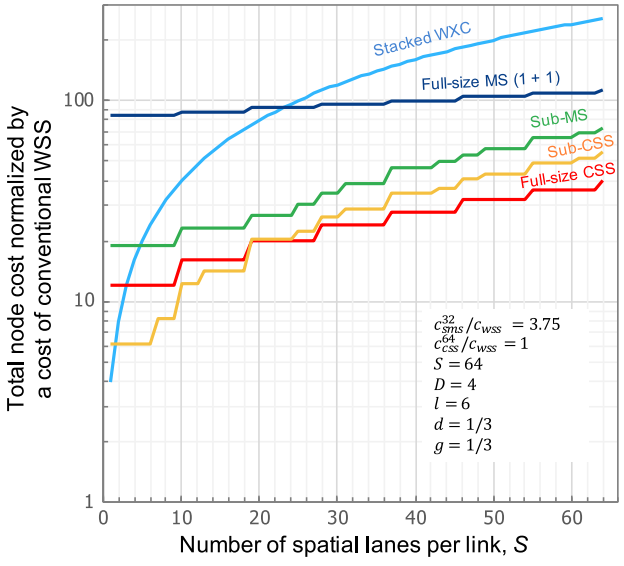

Fig. 10. Total node costs normalized by the cost of a conventional WSS as a function of the number of spatial lanes per link, S.

with that for the baseline single-layer stacked WXC architecture given by Eq. (8). Here, we assume $c_{ms}^{32}/c_{wss} = 3.75$, $c_{css}^{64}/c_{wss} = 1$, $S_{max} = 64$, $D = 4$, $d = 1/3$, $g = 1/3$, $p = 1$, and $q = 0.2$. As expected, the total cost of the baseline single-layer stacked WXC architecture C_{wss} linearly increases with the number of SLs S at the fastest pace. The full-size MS-based HOXC architecture requires the highest initial cost, which corresponds to the costs for two 342×342 MSs and one WXC and increases or decreases depending on the values c_{ms}^{32}/c_{wss} and p. Every time S increases by 9 $(= 1/dg)$, this architecture requires an additional WXC, and then an additional D WSSs.

The sub-MS-based HOXC architecture mitigates the requirement for the initial cost at the expense of reduced connection flexibilities; it provides partial AC and partial LC capabilities. In order to accommodate each line-side input/output fiber pair among D pairs in a WXC by a different sub-MS, we need D sub-MSs at the time of system deployment. We assume $l = 6$; this means we employ a 32×32 MS as a sub-MS. This initial system configuration can support SLs per link S up to 24 $(= lD)$ and after that point an additional sub-MS is required every time S increases by 6 $(= l)$. An additional WXC is also needed every time S increases by 9 $(= 1/dg)$.

If our assumption of $c_{css}^{64}/c_{wss} = 1$ is reasonable, the full-size CSS-based HOXC architecture yields further cost savings as shown in Fig. 10 (red line), although further connection constraints (dedicated core access and no LC) are imposed. As in the case of full-size MSs, every time S increases by 9 $(= 1/dg)$, an additional WXC is required. If a sub-CSS is available at considerably lower cost ($q \ll 1$) than that of a full-size CSS, the sub-CSS-based architecture reduces the initial cost further as shown in Fig. 10 (yellow line) without any penalty to the connection flexibility; however, too small a sub-CSS increases the final cost and may diminish the advantage of its enhanced growability in terms of the number of sub-CSSs.

When HOXCs are fully implemented, relative costs to the single-layer stacked WXC architecture C_{wss} for the HOXC architectures employing SXCs shown in Figs. 7–10 are given by $C_{fms}/C_{wss} = 0.44$, $C_{sms}/C_{wss} = 0.29$, $C_{fcss}/C_{wss} = 0.16$, and $C_{scss}/C_{wss} = 0.22$, respectively. These results indicate that all of the HOXC architectures are much more cost-effective than the single-layer stacked ROADM/WXC architecture. Naturally, dg gives the reachable minimum relative cost and $dg = 0.11$ in this case. The relative cost of C_{fms} is the highest among HOXC architectures investigated in this paper due to the necessity of doubling the cost of an MS for the 1 + 1 MS protection.

V. Conclusions and Remarks

In this paper, we investigated a hierarchical optical network architecture as a promising and practical one to achieve growable, reliable, and cost-effective optical networks in the future massive SDM era. We presented a definition of an SCN architecture with an SCh in the SDM layer, where OChs accommodated in an express SCh bypass the overlying WXCs by using SXCs on the route. Thanks to the potential low-loss feature of SMUX/SDEMUX and spatial switches, we expect that the optical reach of spectrally groomed OChs will remain at almost the same level as that for an OCh transported through a conventional single-layer WDM network, while the optical reach for the spatially bypassed OCh will significantly increase up to 2.3-fold. We proposed two SXC architectures based on sub-MSs and CSSs that support the fault-independent SCh protection covering both the SDM link and spatial switch failures. Simple cost assessment showed that the proposed SXC architectures are more cost-effective than the traditional full-size MS based architecture or stacked ROADM/WXC architecture, although more thorough analysis in terms of trade-off identifications between switch complexity, available connection flexibility, and system cost will be required.

There remain important challenges that have not been discussed in this paper but should be addressed to achieve flexible and operational SCNs. One important question is how to achieve a flexible add/drop part with functionalities of AC, DL, and CL features in a highly cost-effective manner. There must be a wide variety of add/drop part architectures and technologies to achieve these features. We proposed a CSS as a novel key building block for an SXC. We need to establish technologies to make low-loss, compact, and low-cost CSSs. Network design, planning, and control issues such as developing efficient multi-layer routing and resource assignment algorithms as well as migration scenarios from current WDM networks are other important challenges in future SCNs.

Acknowledgment

This work was supported in part by the JSPS KAKENHI Grant Numbers 26220905 and JP18H01443 and the National Institute of Information and Communication Technology (NICT) Grant Numbers 19302 and 20401.

References

[1] P. J. Winzer, "Scaling optical fiber networks: challenges and solutions," *Opt. Photon. News*, vol. 26, no. 3, pp. 28–35, Mar. 2015.

[2] D. M. Marom and M. Blau, "Switching solutions for WDM-SDM optical networks," *IEEE Commun. Mag.*, vol. 53, no. 2, pp. 60–68, 2015.

[3] M. D. Feuer, L. E. Nelson, K. S. Abedin, X. Zhou, T. F. Taunay, J. F. Fini, B. Zhu, R. Isaac, R. Harel, G. Cohen, and D. M. Marom, "ROADM system for space division multiplexing with spatial superchannels," in *Optical Fiber Communication Conf. (OFC)*, 2013, paper PDP5B.8.

[4] L. E. Nelson, M. D. Feuer, K. Abedin, X. Zhou, T. F. Taunay, J. M. Fini, B. Zhu, R. Isaac, R. Harel, G. Cohen, and D. M. Marom, "Spatial superchannel routing in a two-span ROADM system for space division multiplexing," *J. Lightwave Technol.*, vol. 32, no. 4, pp. 783–789, 2014.

[5] N. K. Fontaine, T. Haramaty, R. Ryf, H. Chen, L. Miron, L. Pascar, M. Blau, B. Frenkel, L. Wang, Y. Messaddeq, S. LaRochelle, R. J. Essiambre, Y. Jung, Q. Kang, J. K. Sahu, S. U. Alam, D. J. Richardson, and D. M. Marom,

"Heterogeneous space-division multiplexing and joint wavelength switching demonstration," in *Optical Fiber Communication Conf. (OFC)*, 2015, paper Th5C.5.

[6] M. Jinno and Y. Mori, "Unified architecture of an integrated SDM-WSS employing a PLC-based spatial beam transformer array for various types of SDM fibers," *J. Opt. Commun. Netw.*, vol. 9, no. 2, pp. A198–A206, 2017.

[7] Y. Mori, K. Yamashita, and M. Jinno, "Feasibility demonstration of integrated fractional joint switching WSS applicable for few-mode multicore fiber," in *Photonics in Switching and Computing (PSC)*, 2018, paper Fr3C.3.

[8] Y. Iwai, H. Hasegawa, and K. Sato, "A large-scale photonic node architecture that utilizes interconnected OXC subsystems," *Opt. Express*, vol. 21, no. 1, pp. 478–487, 2013.

[9] M. Niwa, Y. Mori, H. Hasegawa, and K. Sato, "Tipping point for the future scalable OXC: what size M × M WSS is needed?" *J. Opt. Commun. Netw.*, vol. 9 no. 1, pp. A18–A25, 2017.

[10] R. Hashimoto, S. Yamaoka, Y. Mori, H. Hasegawa, K. Sato, K. Yamaguchi, K. Seno, and K. Suzuki, "First demonstration of subsystem-modular optical cross-connect using single-module 6 × 6 wavelength-selective switch," *J. Lightwave Technol.*, vol. 36, no. 7, pp. 1435–1442, 2018.

[11] N. Nemoto, Y. Ikuma, K. Suzuki, O. Moriwaki, T. Watanabe, M. Itoh, and T. Takahashi, "8×8 wavelength cross connect with add/drop ports integrated in spatial and planar optical circuit," in *European Conf. and Exhibition on Optical Communication (ECOC)*, 2015, paper Tu.3.5.1.

[12] D. Klonidis, F. Cugini, O. Gerstel, M. Jinno, V. Lopez, E. Palkopoulou, M. Sekiya, D. Siracusa, G. Thouénon, and C. Betoule, "Spectrally and spatially flexible optical network planning and operations," *IEEE Commun. Mag.*, vol. 53, no. 2, pp. 69–78, 2015.

[13] R. Proietti, L. Liu, R. P. Scott, B. Guan, C. Qin, T. Su, F. Giannone, and S. J. B. Yoo, "3D elastic optical networking in the temporal, spectral, and spatial domains," *IEEE Commun. Mag.*, vol. 53, no. 2, pp. 79–87, 2015.

[14] A. A. M. Saleh, "Transparent optical networking in backbone networks," in *Optical Fiber Communication Conf. (OFC)*, Baltimore, MD, Mar. 7, 2000, paper ThD7.

[15] E. Modiano and A. Narula-Tam, "Mechanisms for providing optical bypass in WDM-based networks," *Opt. Netw. Mag.*, vol. 1, no. 1, pp. 9–16, Jan. 2000.

[16] J. Berthold, A. A. M. Saleh, L. Blair, and J. M. Simmons, "Optical networking: past, present, and future," *J. Lightwave Technol.*, vol. 26, no. 9, pp. 1104–1118, 2008.

[17] M. Jinno, H. Takara, B. Kozicki, Y. Tsukishima, Y. Sone, and S. Matsuoka, "Spectrum-efficient and scalable elastic optical path network: architecture, benefits, and enabling technologies," *IEEE Commun. Mag.* vol. 47, no. 11, pp. 66–73, 2009.

[18] M. Jinno, B. Kozicki, H. Takara, A. Watanabe, Y. Sone, T. Tanaka, and A. Hirano, "Distance-adaptive spectrum resource allocation in spectrum-sliced elastic optical path network," *IEEE Commun. Mag.*, vol. 48, no. 8, pp. 138–145, 2010.

[19] M. Jinno, "Elastic optical networking: roles and benefits in beyond 100-Gb/s era," *J. Lightwave Technol.*, vol. 35, no. 5, pp. 1116–1124, 2017.

[20] G. Baxter, S. Frisken, D. Abakoumov, H. Zhou, I. Clarke, A. Bartos, and S. Poole, "Highly programmable wavelength selective switch based on liquid crystal on silicon switching elements," in *Optical Fiber Communication Conf. (OFC)*, 2006, paper OTuF2.

[21] K. Harada, K. Shimizu, and T. Kudou, "Hierarchical optical path cross-connect systems for large scale WDM networks," in *Optical Fiber Communication Conf./Int. Conf. Integrated Optics and Optical Fiber Communication (OFC/IOOC)*, 1999, vol. 2, pp. 356–358.

[22] M. Jinno, J. Kani, and K. Oguchi, "Ultra-wide-band WDM networks and supporting technologies," in *Core Networks and Network Management (NOC '99)*, 1999, pp. 90–97.

[23] A. A. M. Saleh and J. M. Simmons, "Architectural principles of optical regional and metropolitan access networks," *J. Lightwave Technol.*, vol. 17, no. 12, pp. 2431–2448, 1999.

[24] X. Cao, V. Anand, and C. Qiao, "Framework for waveband switching in multigranular optical networks: part I-multigranular cross-connect architectures," *J. Opt. Netw.*, vol. 5, no. 12, pp. 1043–1055, 2006.

[25] K. Ishii, H. Hasegawa, K. Sato, M. Okuno, S. Kamei, and H. Takahashi, "An ultra-compact waveband cross-connect switch module to create cost-effective multi-degree reconfigurable optical node," in *European Conf. and Exhibition on Optical Communication (ECOC)*, 2009, paper 4.2.2.

[26] M. Cvijetic, I. B. Djordjevic, and N. Cvijetic, "Dynamic multi-dimensional optical networking based on spatial and spectral processing," *Opt. Express*, vol. 20, no. 8, pp. 9144–9150, 2012.

[27] N. Amaya, M. Irfan, G. Zervas, R. Nejabati, D. Simeonidou, J. Sakaguchi, W. Klaus, B. J. Puttnam, T. Miyazawa, Y. Awaji, N. Wada, and I. Henning, "Fully-elastic multi-granular network with space/frequency/time switching using multi-core fibres and programmable optical nodes," *Opt. Express*, vol. 21, no. 7 pp. 8865–8872, 2013.

[28] G. M. Saridis, B. J. Puttnam, R. S. Luis, W. Klaus, T. Miyazawa, Y. Awaji, G. Zervas, D. Simeonidou, and N. Wada, "Experimental demonstration of a flexible filterless and bidirectional SDM optical metro/inter-DC network," in *European Conf. on Optical Communication (ECOC)*, 2016, paper M.1.F.3.

[29] P. J. Winzer and D. T. Neilson, "From scaling disparities to integrated parallelism: a decathlon for a decade," *J. Lightwave Technol.*, vol. 35, no. 5, pp. 1099–1115, 2017.

[30] M. Jinno, "Spatial channel network (SCN) architecture employing growable and reliable spatial channel cross-connects toward massive SDM era," in *Photonics in Switching and Computing (PSC)*, 2018, paper Fr3C.5.

[31] S. Chandrasekhar, X. Liu, B. Zhu, and D. W. Peckham, "Transmission of a 1.2-Tb/s 24-carrier no-guard-interval coherent OFDM superchannel over 7200-km of ultra-large-area fiber," in *European Conf. and Exhibition on Optical Communication (ECOC)*, 2009, paper PD2.6.

[32] P. Poggiolini, "The GN model of non-linear propagation in uncompensated coherent optical systems," *J. Lightwave Technol.*, vol. 30, no. 24, pp. 3857–3879, 2012.

[33] P. Poggiolini, G. Bosco, and A. Carena, "The LOGON strategy for low-complexity control plane implementation in new-generation flexible networks," in *Optical Fiber Communication Conf. (OFC)*, 2013, paper OW1H.3.

[34] M. Jinno, "Added value of introducing spatial bypass into WDM/SDM networks: Gaussian-noise model analysis for spatially-bypassed and spectrally-groomed optical channels," in *European Conf. and Exhibition on Optical Communication (ECOC)*, 2018, paper We3D.6.

[35] O. Shimakawa, M. Shiozaki, T. Sano, and A. Inoue, "Pluggable fan-out realizing physical-contact and low coupling loss for multi-core fiber," in *Optical Fiber Communication Conf. (OFC)*, 2013, paper OM3I.2.

[36] K. Watanabe and T. Saito, "Compact fan-out for 19-core multi-core fiber, with high manufacturability and good optical properties," in *Opto-Electronics and Communications Conf. (OECC)*, 2015.

[37] J. M. Simmons, *Optical Network Design and Planning*, 2nd ed. Springer, 2013.

Masahiko Jinno (M'90–SM'12) received a B.E. degree and M.E. degree in electronics engineering from Kanazawa University, Ishikawa, Japan, in 1984 and 1986, respectively, and a Ph.D. degree in engineering from Osaka University, Osaka, Japan, in 1995 for his work on ultra-fast optical signal processing based on nonlinear effects in optical fibers. He currently serves as a Professor of the Faculty of Engineering and Design at Kagawa University, Takamatsu, Japan. His current research interests include architecture, design, management, and control of optical networks, optical transmission systems, optical cross-connects, optical switches, and rate- and format-flexible optical transponders. Prior to joining Kagawa University in October 2012, he was a Senior Research Engineer and Supervisor at Nippon Telegraph and Telephone (NTT) Network Innovation Laboratories, NTT Corporation conducting pioneering research on spectrum- and energy-efficient elastic optical networks (EONs). From 1993 to 1994, he was a guest scientist at the National Institute of Standards and Technology (NIST), Boulder, Colorado, USA. He has authored or co-authored over 180 peer-reviewed journal and conference papers in the fields of ultra-fast optical signal processing for high-capacity optical time-division multiplexed transmission systems, optical sampling, and optical time-domain reflectometry, ultra-wideband DWDM transmission systems in the L band and S band, ROADM systems, GMPLS and application-aware optical networking, EONs, and SDM networks. Prof. Jinno is a Fellow of the Institute of Electronics, Information and Communication Engineers (IEICE), a senior member of The Institute of Electrical and Electronics Engineers (IEEE), and a member of The Optical Society (OSA). He received the Young Engineer's Award in 1993, the Best Tutorial Paper Award in 2011, the Best Paper Award in 2012, the Achievement Award in 2017, and a Milestone Certificate in 2017 from the IEICE; the Best Paper Awards from the 1997, 1998, and 2007 Optoelectronics and Communications Conferences (OECC); the Best Paper Award from the 2010 ITU-T Kaleidoscope Academic Conference; and the Outstanding Paper Award in 2013 from the IEEE Communications Society Asia-Pacific Board.